Smart Structures and Systems, *Vol. 18, No. 3 (2016) 625-642*
DOI: http://dx.doi.org/10.12989/sss.2016.18.3.625

Experimental validation of smartphones for measuring human-induced loads

Jun Chen*, Huan Tan[a] and Ziye Pan[b]

Department of Structural Engineering, Tongji University, No.1239 Siping Road, Yangpu District, Shanghai, China

(Received May 30, 2015, Revised August 15, 2015, Accepted August 20, 2015)

Abstract. The rapid technology developments in smartphones have created a significant opportunity for their use in structural live load measurements. This paper presents extensive experiments conducted in two stages to investigate this opportunity. Shaking table tests were carried out in the first stage using selected popular smartphones to measure the sinusoidal waves of various frequencies, the sinusoidal sweeping, and earthquake waves. Comparison between smartphone measurements and real inputs showed that the smartphones used in this study gave reliable measurements for harmonic waves in both time and frequency domains. For complex waves, smartphone measurements should be used with caution. In the second stage, three-dimensional motion capture technology was employed to explore the capacity of smartphones for measuring the movement of individuals in walking, bouncing and jumping activities. In these tests, reflective markers were attached to the test subject. The markers' trajectories were recorded by the motion capture system and were taken as references. The smartphone measurements agreed well with the references when the phone was properly fixed. Encouraged by these experimental validation results, smartphones were attached to moving participants of this study. The phones measured the acceleration near the center-of-mass of his or her body. The human-induced loads were then reconstructed by the acceleration measurements in conjunction with a biomechanical model. Satisfactory agreement between the reconstructed forces and that measured by a force plate was observed in several instances, clearly demonstrating the capability of smartphones to accurately assist in obtaining human-induced load measurements.

Keywords: human-induced load; smartphone; shaking table; motion capture technology; measurement

1. Introduction

Due to their lightweight and flexibility, footbridges, large-span floors and cantilever grandstand structures are very often prone to human-induced vibrations (Brownjohn *et al.* 2004). Predicting the dynamic response of these structures due to human-induced loading has therefore become a critical aspect of vibration serviceability evaluation (Van Nimmen *et al.* 2014). Better knowledge of the dynamic properties of crowd-induced loading was the key issue for this evaluation. The traditional direct force measurements utilize an instrumented treadmill or force plates integrated in

*Corresponding author, Professor, E-mail: cejchen@tongji.edu.cn
[a] Ph.D. Candidate, E-mail: 08yvonnetan@tongji.edu.cn
[b] Master Student, E-mail: lizzie.feehily@foxmail.com

http://www.techno-press.org/?journal=sss&subpage=8 ISSN: 1738-1584 (Print), 1738-1991 (Online)

the walkway (Dierick *et al.* 2004). This methodology, however, is not suitable for measuring the crowd-induced force. Another common method is to use cameras or a digital head-tracking system to record the movement of individuals in a crowd (Fujino *et al.*1993, Yoshida *et al.* 2007, Araújo *et al.* 2009). Recently, newly emerged measurement technologies in biomechanical science have been adopted to investigate human-induced loads, such as the optical marker-based technology of Vicon (Wang *et al.* 2011) and CODA (Richards 1999). However, due to the limited number of instruments available and limitation on the measurement range, the problem of how to measure crowd-induced dynamic loading properties in an effective and easy-to-apply manner is still a challenging issue.

Nowadays, smart mobile phones (hereafter referred to as smartphones) are widely used on a daily basis. With the rapid development of micro-chip technology, a tri-axial accelerometer and a tri-axial gyroscope based on MEMS (Micro-Electro-Mechanical system) have been integrated into smartphones, which provide a good technical platform for implementation (Spencer 2003;). Smartphone development continues to serve a fast growing and broad variety of applications including remote medical treatment (Cao *et al.* 2009, Lau *et al.* 2010), remote home automation and security monitoring (Zhang *et al.* 2007), and especially for human activity monitoring and education in medical healthcare applications (Khan *et al.* 2010, Lee and Cho 2011, Wu 2012). One of the most recent developments has been in the field of structural health monitoring (Yu *et al.* 2015, Feng *et al*. 2015).

Smart phones as daily-used and portable electronic devices are capable of recording the kinetics of individuals in a crowd. Considering the merits of smartphones with built-in tri-axial accelerometers, it is of great significance to investigate the possibility of using smartphones as a ‘mobile vibration measurement device’ to measure human-induced loads such as the walking load, bouncing load and jumping load. The purpose of this paper is, therefore, to verify the possibility, capacity and accuracy of smartphones for human-induced loads measurements by extensive experiments.

2. Smartphones

2.1 Selection of smartphones and software

Preliminary tests using a small-scale shaking table were performed in order to select proper smartphones and data acquisition software from many software providers. In total, seven smartphones from four market-leading brands and three software applications were tested which are listed in Table 1. The test arrangement is shown in Fig. 1. The seven smartphones have two operating systems. By comparing each smartphone’s measurement with the shaking table’s input, we finally selected the iPhone 4s (and higher generations) manufactured by Apple Inc. and Sensorlog® as the hardware and software, respectively, for the following experiments. The iPhone manufactured by Apple Inc. was the first to integrate tri-axial accelerometers and gyroscopes based on MEMS into phones, and this is why we selected iPhone 4s as the first phone to test. The iPhone’s market popularity is another important factor if we want to apply it to crowd load measurement and to future anonymous individual loads collection. A mobile phone application software, Sensorlog, was selected as the data acquisition software because it is free and has the highest sampling rate of 100 Hz compared with other analogous apps. The iPhone’s built-in sensor unit (inclination, gyro, GPS, and acceleration) is used for monitoring an object’s original motion

information. The information is then processed and analyzed through the self-developed intelligent algorithm embedded in the iPhone. Sensorlog is able to provide information concerning latitude and longitude, acceleration in local coordinates of iPhone and the raw gyro rotation rate of the phone with the maximum sample frequency of 100 Hz. The main interface of the Sensorlog is shown in Fig. 2.

Table 1 Smartphones' built in accelerometer sensors

Phone type	Accelerometer Model	Manufacturer	Quantity Measured	Apps
iPhone 4s	LIS331DLH	ST Microelectronics	Acceleration	(1) Sensorlog; (2) Sensor kinetics;
iPhone5	STM33DH	ST Microelectronics	Acceleration	
iPhone5s	BMA 220	Bosch	Acceleration	
iPhone6	BMA 280/ MPU-6700	Bosch/ InvenSense	Acceleration& Angular velocity	
GALAXY Note 3	MPU-6500	InvenSense	Acceleration & Angular velocity	(1) Sensor kinetics; (2) AndroSensor;
Xiao Mi 3	MPU6050	InvenSense	Acceleration	
HTC ONE	Unknown	-	-	

Fig. 1 The experimental setup

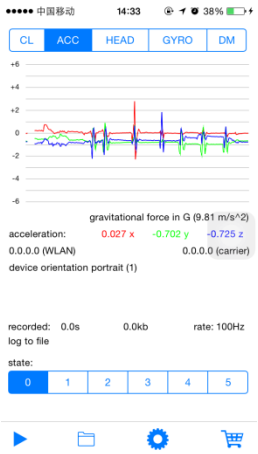

Fig. 2 The interface of Sensorlog®

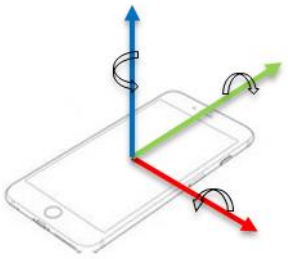

Fig. 3 Local coordinates of embedded accelerometer and tri-axial gyroscope

2.2 Vibration measurement by smartphone

Fig. 3 shows the local coordinates and positive directions of a smartphone's embedded tri-axial accelerometer and tri-axial gyroscope. The plane that consists of x and y axes is parallel to the smartphone's screen. The embedded accelerometer is able to record acceleration in x , y , and z directions which are mutually perpendicular, while the tri-axial gyroscope can record the angular rotation velocity ($\theta_x, \theta_y, \theta_z$, units: rad/s) of these three axes. To measure the movement of an object, the smartphone can be fixed on object so that one of the three axes, say the x axis, of phone is in the same direction as the vibration. Under such a circumstance, the smartphone's acceleration measurement in x direction represents the object's movement in that direction.

When using the smartphones for human-induced load measurement, usually we know the orientation of its local coordinates at the beginning (t = 0), e.g., x-axis is perpendicular to the ground and y-axis is parallel to the ground, which is then defined as the reference coordinate or the global coordinate. During the measurement, the orientation of the smartphone's local coordinates is changing due to the movement and rotation of human body. Therefore, we need coordinate

transformation rules to convert smartphone measurements at any time instant *t* from local coordinates to the global coordinates.

Assume the accelerations recorded by the smartphone at time instant *t* are $a_1(t), a_2(t)$ and $a_3(t)$ in the local coordinates. The accumulated angles of rotation about the three axes from time 0 to *t* are as follows

$$\alpha_t = \sum_1^n \theta_x \Delta t;\ \beta_t = \sum_1^n \theta_y \Delta t;\ \gamma_t = \sum_1^n \theta_z \Delta t \tag{1}$$

in which *n* means the total number of sample points up to time *t*. The following equation is used to transfer $a_1(t)$, $a_2(t)$ and $a_3(t)$ to the global coordinates

$$\left[a_x(t), a_y(t), a_z(t)\right]^T = H * \left[a_1(t), a_2(t), a_3(t)\right]^T \tag{2}$$

in which the transformation matrix *H* is

$$H = \begin{bmatrix} \cos\beta\cos\gamma & \sin\alpha\sin\beta+\cos\alpha\cos\gamma & \sin\alpha\sin\gamma-\cos\alpha\sin\beta\cos\gamma \\ -\cos\beta\sin\gamma & \cos\alpha\cos\gamma-\sin\alpha\sin\beta\sin\gamma & \sin\alpha\cos\gamma-\cos\alpha\sin\beta\sin\gamma \\ \sin\beta & -\sin\alpha\cos\beta & \cos\alpha\cos\beta \end{bmatrix} \quad \text{n} \tag{3}$$

Eq. (2) transfers the acceleration measured by the smartphone at any time instant t to the reference coordinates at the beginning of the measurement.

3. Calibration tests using a shaking table

3.1 Experimental setup

Vibration serviceability problems in long-span structures, i.e., pedestrian bridges, floors and cantilever grandstands, are mostly caused by people walking, bouncing or jumping. Thus, the experimental tests were focused on these three types of human-induced load, which is a near-periodic process and is characterized by its frequency, amplitude and phase. The frequency range of walking is from 1.5 to 2.5 Hz and that of jumping or bouncing is normally between 2.5 and 3.5 Hz.

In the shaking table experiment, smartphones were fixed on an organic glass which was in turn fixed by bolts on a small scale shaking table manufactured by Quanser Co. (Fig. 1). Different inputs were introduced to the shaking table, including sinusoidal waves of different frequencies, sweep waves and earthquake waves. The measurement accuracy of the smartphones is designed to be identical in every axis since the same MEMS chip is utilized and fully differential capacitive sensing and common-centroid configurations are realized in all the axes. Therefore, only the x-axis was tested in the experiments. Amplitude controlling strategy was adopted in the test that the shaking table had constant vibration amplitude for each case. A dual-axis ADXL210E accelerometer was embedded in the shake table to measure the acceleration of the platform in both x and y directions. The sensor has a measurement range of ±10 g, and its noise level in the operation range of the shake table is approximately ±5.0 mV, i.e. ±5.0 mg. The record of the embedded accelerometer was taken as a reference to verify records from smartphones.

3.2 Sinusoidal wave

Eight sinusoidal waves were tested in the experiments. Their frequencies ranged from 1.2 to 3.4 Hz with an interval of 0.4 Hz, covering the typical frequency range of human-induced loads. For test cases with 1.6 and 3.4 Hz sinusoidal waves, Figs. 4(a) and 4(b) compares the time histories and corresponding Fourier amplitude spectra for the smartphone records with that of the reference waves. Visual observation indicates that the records from smartphones are very close to the real waves in both time and frequency domain. To quantify the measurement error, the relative error of each peak in measured and reference time histories were computed. The mean values and standard deviations are presented in Table 2. The last column of Table 2 gives the relative error between the dominating frequency of the smartphone record and the preset frequency in the test. Note that the maximum peak measurement error is lower than 4%, and the difference in dominating frequency is negligible.

3.3 Sinusoidal sweeping wave

In order to verify the smartphones' adaptation to the vibration environment, the sinusoidal sweeping test was also conducted. Normally, a sinusoidal sweeping vibration test is utilized to simulate the devices vibrating condition when the resonant frequency is unable to be determined beforehand. In this experiment, the input to the shaking table was a sine sweeping wave that increased from 1 Hz to 7.5 Hz in 20 seconds. The amplitude of the sweeping wave was set at 2 mm. The test was repeated several times. In each case, the smartphones' records were compared with the output data of the shaking table in terms of time history, Fourier amplitude spectrum and the one-second running root-mean-square (1s-RMS), which was calculated using the time-history. Figs. 5(a) and 5(b) shows the comparison for one test case.

Table 2 Mean values and standard deviation of relative error peak values and frequencies

	Error of peaks		Error of frequency(%)
Cases	Mean (%)	STD(%)	
1.2 Hz	3.59	1.56	0.37
1.6 Hz	2.68	0.97	0.62
2.0 Hz	1.35	0.89	0.99
2.4Hz	0.66	0.35	0.83
2.8 Hz	0.68	0.49	0.12
3.2 Hz	1.08	0.79	0.19
3.4Hz	1.13	0.76	0.29
3.6 Hz	1.55	0.95	0.90

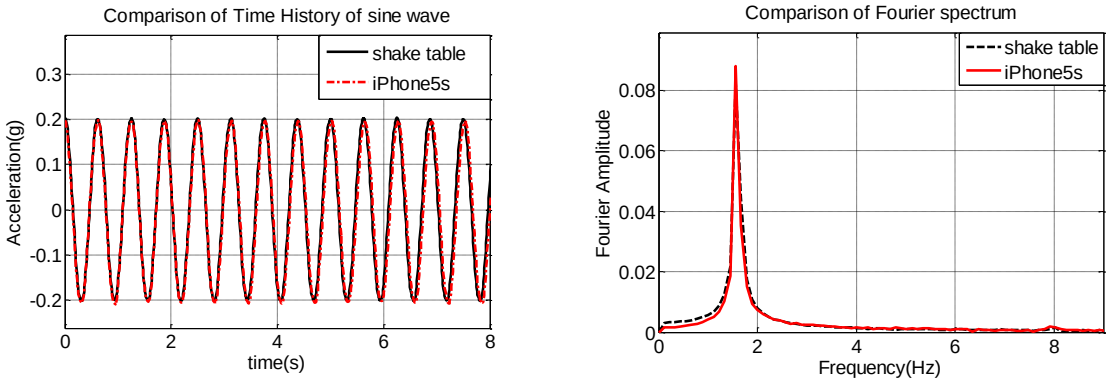

(a) 1.6 Hz

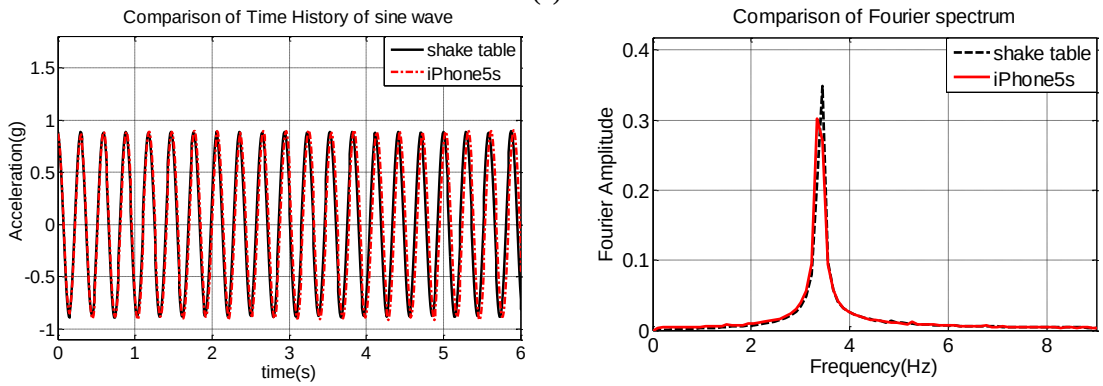

(b) 3.4 Hz

Fig. 4 Time history of sensors under sine wave vibration

As shown in Fig. 5(a), the time history of the smartphone's record is close to the real input, and the 1s-RMS acceleration recorded by the smartphone is slightly larger than that of the reference. The conclusion was the same for the other test cases. For the Fourier amplitude spectrum, the measurement by smartphone was close to that of the real input as demonstrated in Fig. 5(b).

3.4 Earthquake wave

In order to verify the accuracy of smartphone's built-in tri-axial accelerometer to wideband random vibration, we conducted the earthquake wave tests. Four field earthquake records were used as the shaking table's inputs: 1) the El Centro earthquake, 2) the Northridge earthquake, 3) the Kobe earthquake and 4) the Cape Mendocino earthquake data. For the El Centro earthquake, the shaking table's output and three measurements by smart phones are shown in Fig. 6 with their corresponding Fourier amplitude spectra given in Fig. 7.

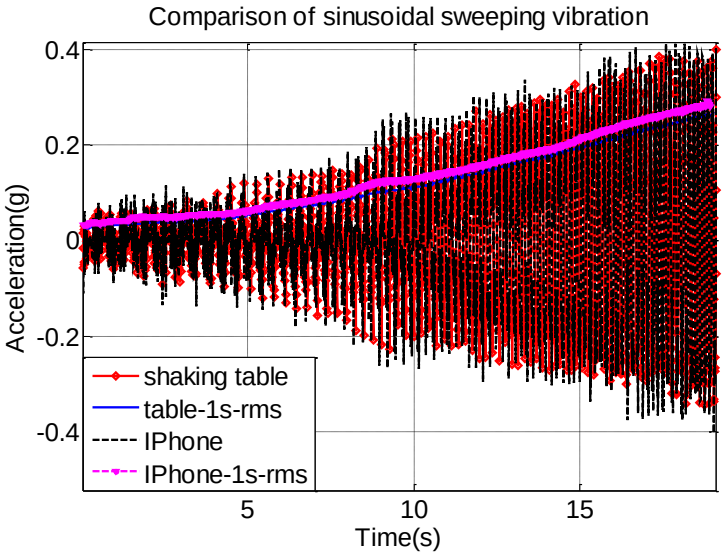

(a) Comparison of time histories and 1s RMS

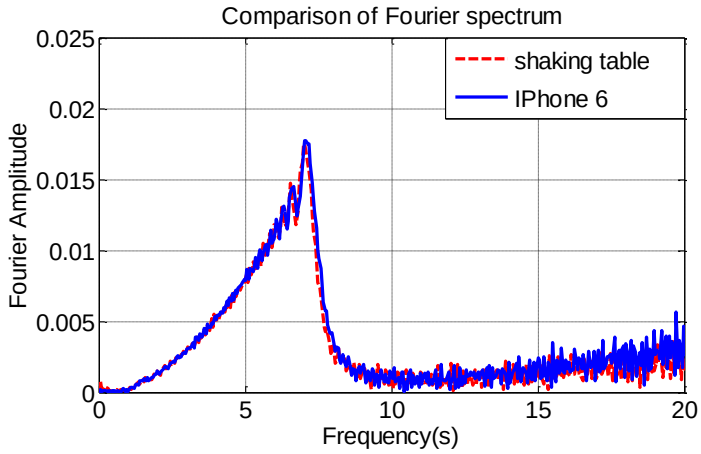

(b) Comparison of Fourier spectrum of iPhone6 and a shaking table

Fig. 5 Comparison of shaking table data and smartphones recording during the sinusoidal sweep vibration

It can be seen that the smartphone measurements are similar to the shaking table vibration in terms of shape of curves, frequencies, and maximum values. However, it should be noted that the peaks in the smartphone records appear at different times from that of the real input. Our experiment results suggest that for complex waves, such as earthquakes that have high frequency components, smartphone records should be used with caution.

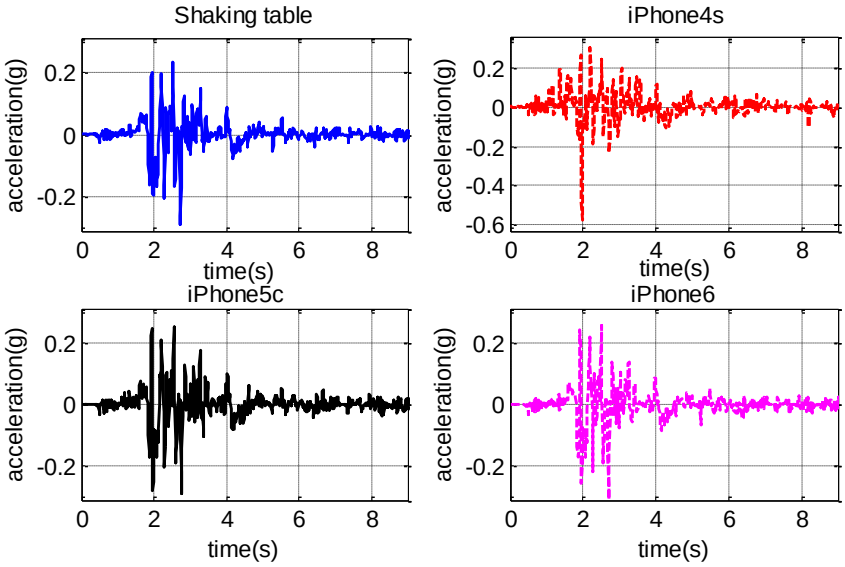

Fig. 6 Comparison of the recorded time histories under the El Centro earthquake vibration

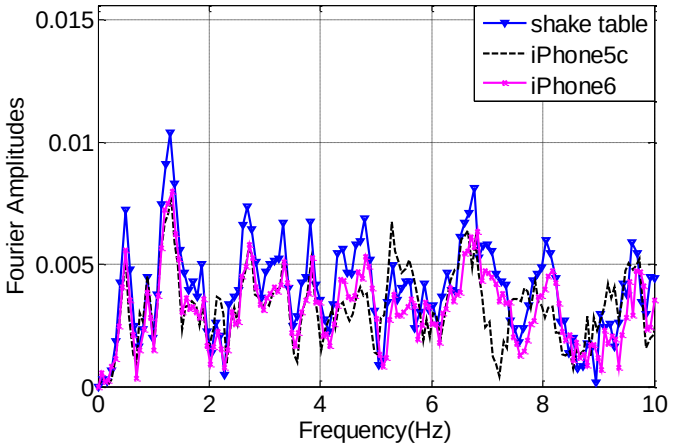

Fig. 7 The Fourier spectrum of the shake table input and smartphones records

4. Calibration tests using motion capture technology

4.1 Experimental setup

The accuracy of selected smartphones for measuring low frequency harmonic waves was validated by the shaking table test. We intend to use smartphones to record people's daily movements and the resulting loads. Since smartphones are carried by people in many different

manners, the effect of smartphone carrying manner for the individual phone carrier can affect measurement results and should be further validated. To this end, we designed and conducted experiments using a three-dimensional motion capture system, which is an advanced measurement technology capable of synchronously recording motions of reflective markers attached to a test subject. The Vicon Motion Capture System was used in the test. It contains 12 infra-red cameras, four fixed force plates, and associated software for data recording and processing, as shown in Fig. 8. The distance measurement accuracy of the system is 0.1 mm. More information about the motion capture technology can be found in Peng *et al*. (2015).

In the experiment, test subjects were asked to wear skinny jeans and performed bouncing, jumping and walking activities. Four reflective markers were attached to the test subject's pelvis as shown in Figs. 8(a) and 8(b). According to the Vicon System's instruction, the average of the four markers' records is very close to the trajectory of COM, which was also proved by previous studies (Zhang *et al*. 2013). Thus, the average value of the four markers' records was taken as the COM's trajectory. After each test, the COM's vertical acceleration was calculated using all the markers' trajectories, and it was then taken as a reference for latter comparison. One additional marker was attached to the smartphone to record its acceleration in the global coordinates of the motion capture system. The trajectory of this special marker was used as a reference to verify the coordinates conversion rules.

4.2 Smartphone carrying manner

To investigate the effect of smartphone carrying manner on the measurement result, we tried two methods: M1) the smartphone was put in the test subject's pocket (Fig. 8(a)), and M2) the smartphone was bound to the test subject's waist by a belt placing the smartphone close to the pelvis (Fig. 8(b)). For each carrying method, the test subject was instructed to conduct jumping, bouncing and walking tests three times at different frequencies instructed by a metronome.

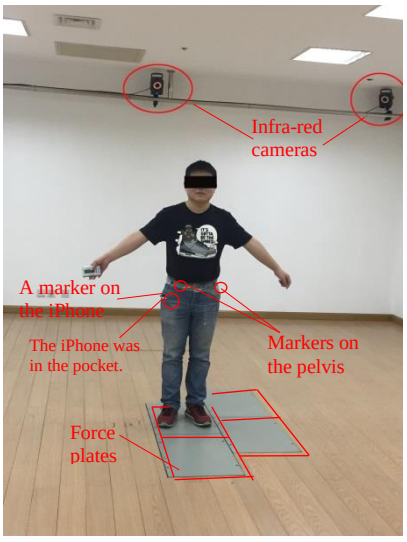

(a) Carrying manner 1

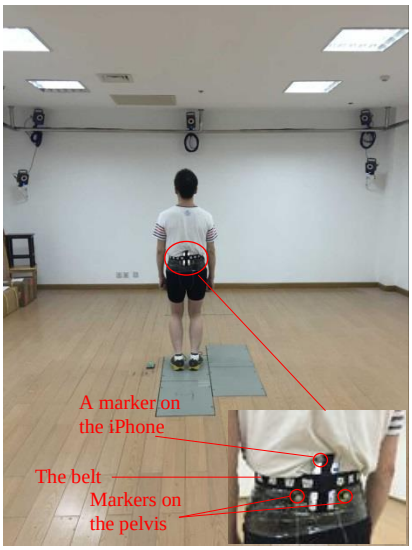

(b) Carrying manner 2

Fig. 8 Two different phone carrying manners in the test

Figs. 9(a) and 9(b) compare the smartphone measurements with the corresponding references for the first carrying manner, and Figs. 10(a) and 10(b) show the results for the second manner. Visual observation suggests that the second carrying manner gives a better measurement than the first one. The conclusion for other test cases is the same. This observation is actually the same as for the traditional accelerometer, which is also required to be securely fastened on the object.

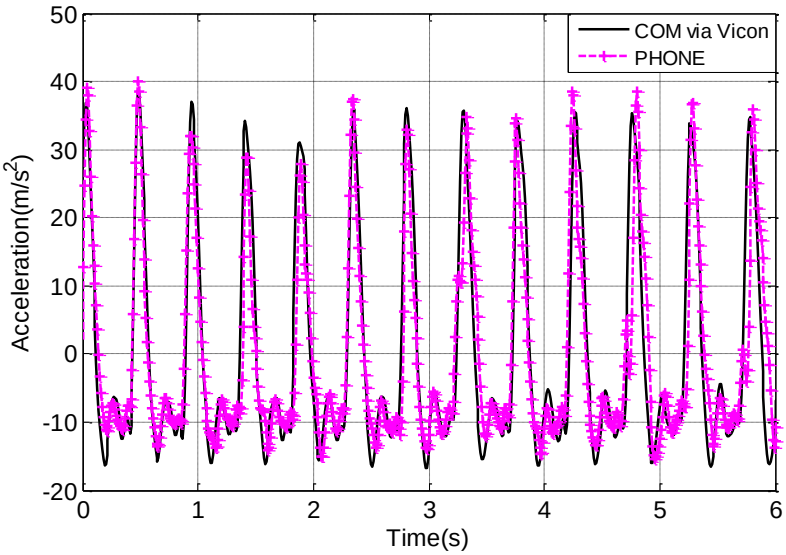

(a) Jumping at 2.0 Hz

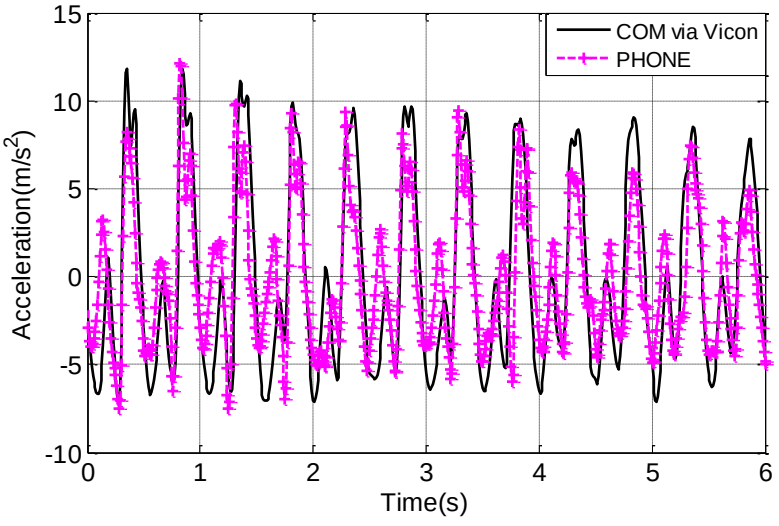

(b) Bouncing at 2.0 Hz

Fig. 9 Comparison of acceleration measurements between iPhone and Vicon (Carrying manner 1)

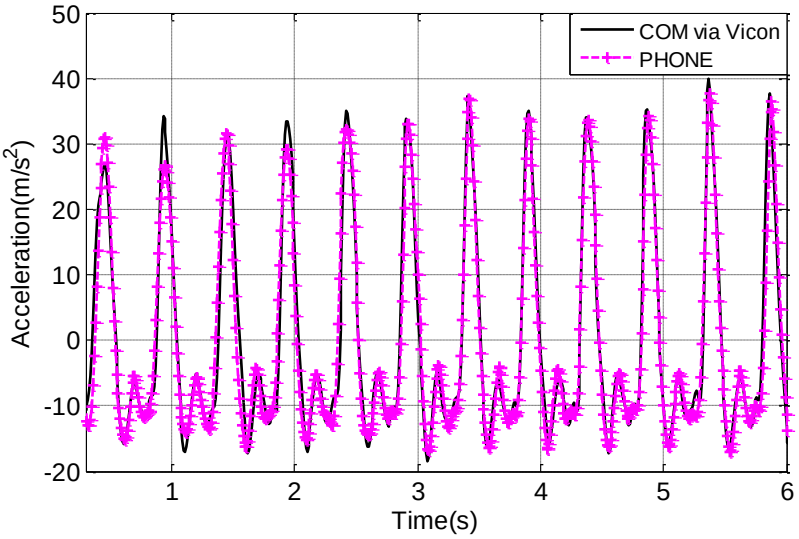

(a) Jumping at 2.0 Hz

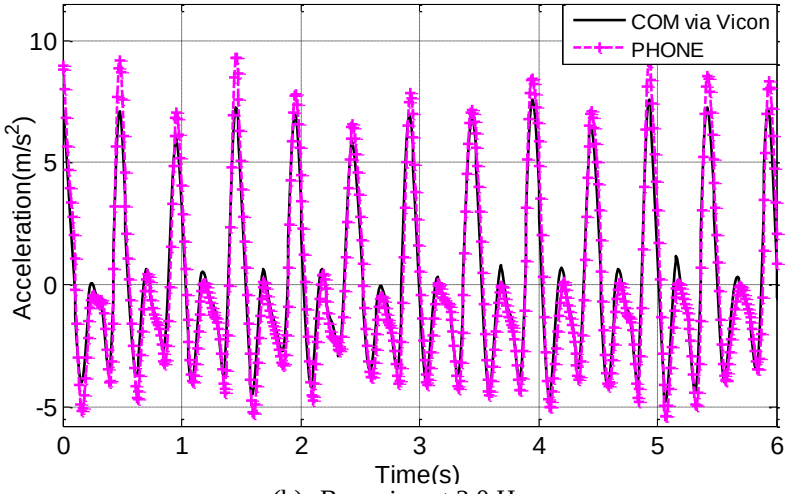

(b) Bouncing at 2.0 Hz

Fig. 10 Comparison of acceleration measurements between iPhone and Vicon (Carrying manner 2)

After comparing the two different carrying manners, it is obvious that when the smartphone was bound close to the test subject's COM, the smartphone measurements are able to represent the trajectories of COM. The second carrying manner is therefore recommended for real application of smartphones for human activity measurements.

4.3 Coordinate conversion

At the beginning of each test, the coordinates of smartphones were set in accordance with that of the motion capture system by fixing the phone at the origin of Vicon's global coordinates and then pressing the start button of Sensorlog. By this means, the smartphone's 'global coordinates' as

defined in section 2.2 were the same as the Vicon System. After each test, Eq. (2) was applied to the smartphone records to convert them from local coordinates to global coordinates. For the bouncing case at 2.6 Hz, Fig. 11(a) compares the original and converted smartphone acceleration measurements with that of the reference marker.

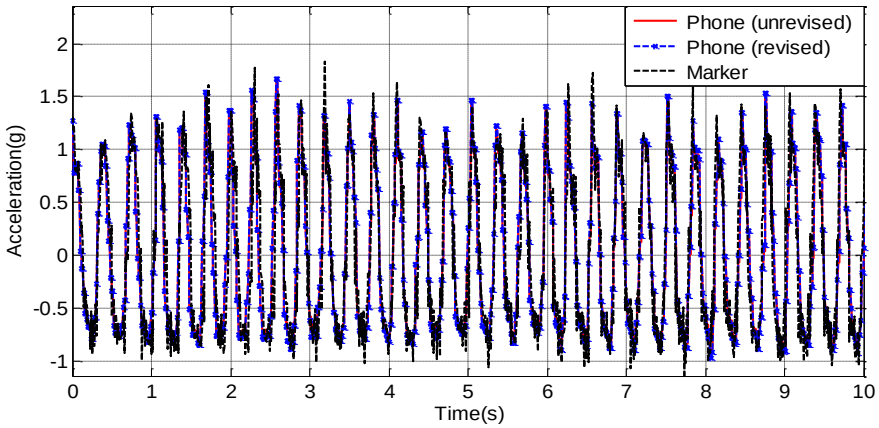

(a) Comparison of acceleration

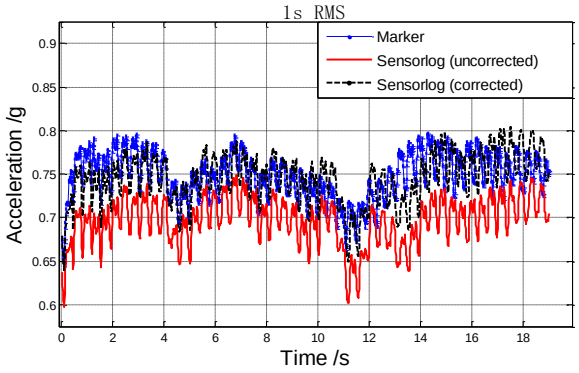

(b) Comparison of 1sRMS values

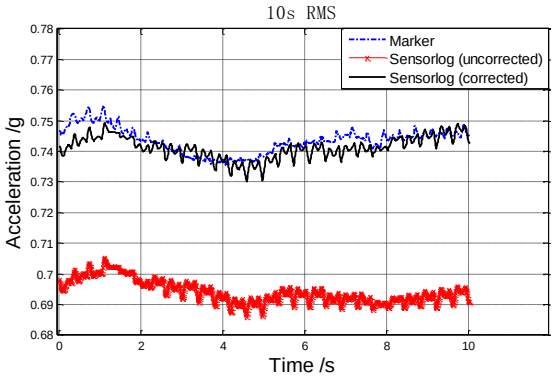

(c) Comparison of 10sRMS values

Fig. 11 Comparison of accelerations of bouncing at 2.6 Hz

Figs. 11(b) and 11(c) further compare the 1s-RMS and 10s-RMS curves of the smartphone records with that of the reference. Note that the acceleration time history, 1s-RMS and 10s-RMS, after revision are much closer to those of the reflective marker. The conclusion for the other test cases is the same.

The above experimental results clearly demonstrate that when applied to human movement measurement, it is very important to set the smartphones' local coordinates to a known direction at the beginning and perform coordinate conversion afterward. Moreover, the smartphone should be securely attached to the object in order to get high quality measurements.

5. Application for human-induced loads measurement

After we attach a smartphone close to a person's COM in a walking/bouncing/jumping activity, the vertical acceleration measured by the smartphone (after coordinates conversion) can represent the acceleration of COM in the vertical direction, which is parallel to gravity. The loads induced by the person's activity can then be computed by introducing COM's acceleration into the biomechanical model of the person (Chen *et al*. 2015). The simplest model is given in Eq. 4, which treats each person as a single rigid body

$$G(t) = mg + ma_{\mathrm{y}} \tag{4}$$

in which $G(t)$ is the ground reaction force (GRF) caused by the person, m is the body mass of the person, g is the gravitational acceleration and a_y is the vertical acceleration of a person's COM. For activity such as bouncing, not all of a person's body mass participates in the vibration; a dynamic participation coefficient was introduced as $R(0 < R \le 1)$ which is the ratio of that part of the mass participating in vibration and the whole human mass. As a result, Eq. (4) is expressed as

$$G(t) = mg + mRa_y \tag{5}$$

We applied Eq. (5) to all the test cases in the motion capture experiments to calculate the ground reaction force. Taking the bouncing experiment as an example, Figs. 12(a) and 12(b) compare the bouncing force measured by the force plate and that obtained by Eqs. (4) and (5). As shown in Fig. 12(a), the single-rigid biomechanical model where R=1 is not good enough to reproduce the ground reaction force. This is because in the bouncing activity, the lower legs of the person don't fully participate in the vibration. With R = 0.7870 in Eq.(5), the reproduced force agrees well with the force plate measurement as shown in Fig. 12(b). The R value was determined by trial and error. Figs. 13(a) and 13(b) give the analogous comparison in bouncing activity at 1.5 Hz. The relative errors in peak and root-mean-square (RMS) were computed between force plate measurements and that obtained by Eqs. (4) and (5). The results are shown in Table 4 with the R values used in the calculation.

Note from Table 3 and 4 that for bouncing and jumping tests, the peak errors vary in a range 6% - 25% and 13% - 32% respectively, while the RMS errors are all lower than 2%. It is worth emphasizing that experimental results in Section 4 already demonstrated that the acceleration recorded by the smartphone is very close to the COM's acceleration; therefore, the errors presented in Table 4 are mainly due to the biomechanical model (Eq. (4) or Eq. (5)). In other words, Table 4 shows that when a proper model is selected, the loads calculated using the smartphone

measurements are acceptable. Our experimental results indicate that the R factor is individual-dependent. The mean values R = 0.76 for bouncing and R = 0.88 for jumping from this study could be options. However, it is beyond the scope of this paper to find a proper R factor for the biomechanical model.

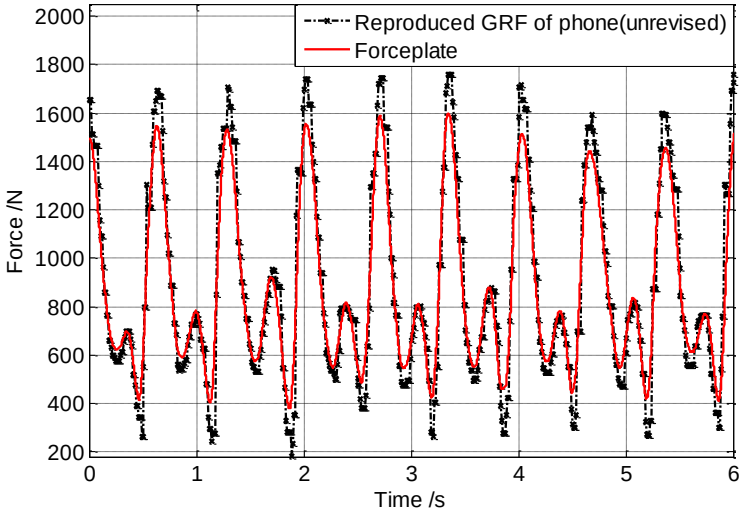

(a) Reproduced GRF using a single-rigid model (R=1)

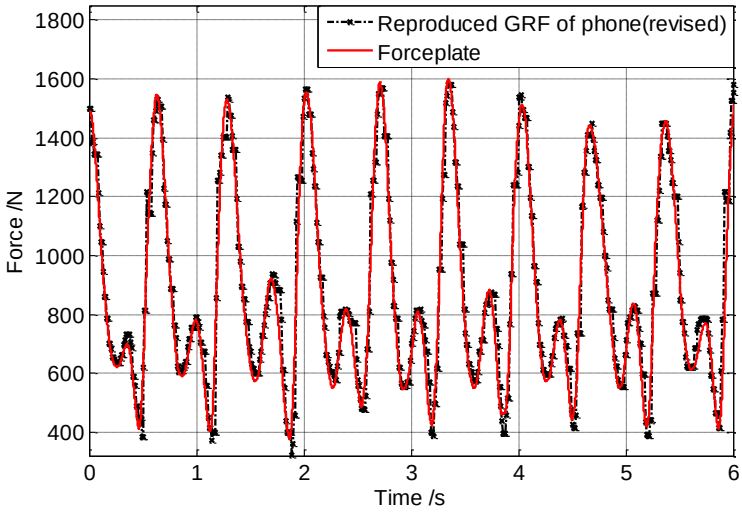

(b) Reproduced GRF using a single-rigid model (R=0.761)

Fig. 12 Comparison of the reproduced GRF with force plate measurement (Bouncing frequency 2 Hz)

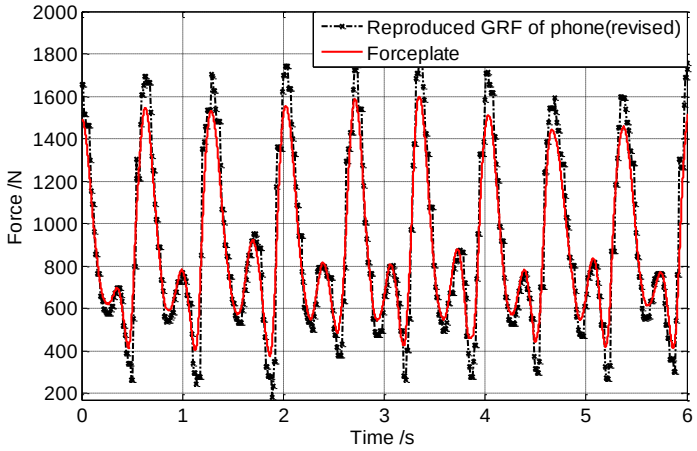

(a) Reproduced GRF with a single-rigid model (R=1)

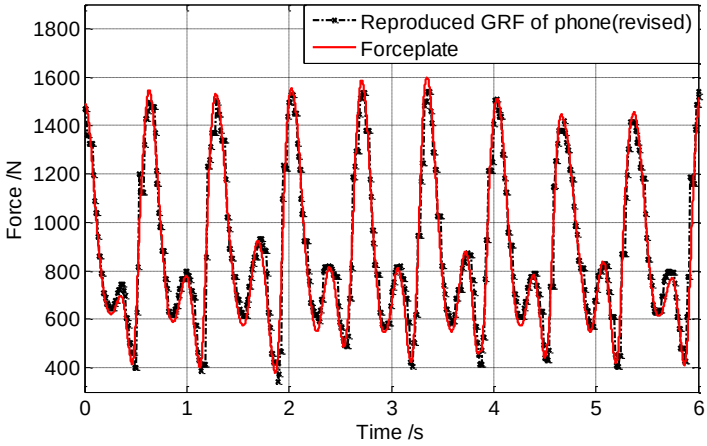

(b) Reproduced GRF with a single-rigid model (R=0.896)

Fig. 13 Comparison of the reproduced GRF with force plate measurement (jumping frequency 1.5 Hz)

Table 3 Errors between reproduced and measured GRF of bouncing load with R for one subject

Cases(Hz)	R = 1		R ≠ 1		
	Peak errors(%)	Errors of RMS(%)	R	Peak errors(%)	Errors of RMS(%)
1.5 Hz	18.15	5.49	0.708	5.7764	0.1
2.0 Hz	20.93	7.14	0.761	8.2965	0.69
2.5 Hz	17.78	6.24	0.853	24.71	1.52
3.2 Hz	26.64	5.63	0.735	14.5845	0.67

Table 4 Errors between reproduced and measured GRF of jumping load with R

Cases(Hz)	R	Peak errors (%)	Errors of RMS (%)
1.5 Hz	0.896	17.37	0.43
2.0 Hz	0.882	13.10	0.30
2.8 Hz	0.907	16.63	0.34
3.5 Hz	0.844	32.43	0.7

6. Conclusions

Based on the experimental results on the selected smartphones and data collection software in this study, the following conclusions and limitations were obtained.

- The selected smartphones (iPhone5c and higher generation) are able to measure simple sinusoidal waves with high accuracy. For complex vibration waves like earthquake waves, the measurement accuracies of the selected smartphones were not up to our standards in the experiments conducted.
- With a secure carrying manner and coordinates revision, the selected smartphones can measure a person's walking, jumping, and bouncing movement with good accuracy.
- The human loads induced by walking, jumping, and bouncing can be computed by introducing the smartphone measurements into a biomechanical model of the moving person. The accuracy of the reproduced load mainly depends on the accuracy of the model.
- This kind of technique is limited because of the smartphone type and software. Even for iPhones which were tested in this paper, different series of phones have different accelerometer sensors so that their accuracy will not all measure out to the same results.
- With the merits of being used daily and their around-the-clock accessibility as portable electronic devices, smartphones tested herein were capable of recording the kinetics of individuals in a crowd and the loading force was estimated conveniently and simply.

Acknowledgements

Financial supports for this paper's research came to the first author, Jun Chen, from the National Natural Science Foundation (51478346) and State Key Laboratory for Disaster Reduction of Civil Engineering (SLDRCE14-B-16). Dr. Chen expresses appreciation for these supports.

References

Araújo, J., Carlos, M. and Brito H.M.B.F. (2009), "Experimental evaluation of synchronization in footbridges due to crowd density", *Struct. Eng. Int.*, **19**(3), 298-303.

Brownjohn, J.M.W., Fok, P. and Roche, M. (2004), "Long span steel pedestrian bridge at Singapore Changi

Airport-Part 1: prediction of vibration serviceability problems", *Struct. Eng.*, **82**(16), 21-27.
Cao, D., Wang, H. and Hu, Y. (2009), "Design and research of remote ECG display system based on smartphone", *J. Xihua U: Nat. Sci. Ed.*, **4**, 005.
Chen, J., Zhang, M.S. and Liu, W. (2015), "Vibration serviceability performance of an externally prestressed concrete floor during daily use and under controlled human activities", *J. Perform. Constr. Fac*.
Chen, J., Zhang, M.S., Zhao, Y.F. and Zhan, H.S. (2014), "Kinematic data smoothing using ensemble empirical mode decomposition", *J. Med. Imag. Health Inform.*, **4**(4), 540-546.
Dierick, F., Penta, M. and Renaut, D. (2004), "A force measuring treadmill in clinical gait analysis", *Gait. Posture.*, **20**(3), 299-303.
Feng, M., Fukuda, Y., Mizuta, M. *et al*. (2015), "Citizen sensors for SHM: use of accelerometer data from smartphones", *J. Sensors*, **15**(2), 2980-2998.
Fujino, Y., Pacheco, B.M., Nakamura, S.I. *et al.* (1993), "Synchronization of human walking observed during lateral vibration of a congested pedestrian bridge", *Earthq. Eng. Struct. D.*, **22**(9), 741-758.
Khan, A.M., Lee, Y.K., Lee, S.Y. *et al.* (2010), "Human activity recognition via an accelerometer-enabled-smartphone using kernel discriminant analysis", *Future Information Technology (FutureTech)*, Busan, Korea, May.
Lau, S.L., König I., David, K. *et al*. (2010), "Supporting patient monitoring using activity recognition with a smartphone", *Wireless Communication Systems (ISWCS), 2010 7th International Symposium on.* IEEE. 810-814.
Lee, Y. and Cho, S. (2011), "Activity recognition using hierarchical hidden markov models on a smartphone with 3D accelerometer", *Hybrid Artificial Intelligent Systems*, Wroclaw, Poland, May.
Littler, J.D. (2003), "Frequencies of synchronised human loading from jumping and stamping". *Struct. Eng.*, **81**(22), 27-35.
Peng, Y.X., Chen, J. and Ding, G. (2015), "Walking load model for single footfall trace in three dimensions based on gait experiment", *Struct. Eng. Mech.*, **54**(5), 937-953.
Richards, J.G. (1999), "The measurement of human motion: a comparison of commercially available systems", *Hum. Movement. Sci*., **18**(5), 589-602.
Spencer, B.F. (2003), "Opportunities and challenges for smart sensing technology", *Structural Health Monitoring and Intelligent Infrastructure*, Tokyo, Japan, November.
Van Nimmen, K., Lombaert, G., Jonkers, I. *et al*. (2014), "Characterization of walking loads by 3D inertial motion tracking", *J. Sound. Vib.*, **333**(20), 5212-5226.
Wang, L., Chen, J. and Peng Y.X. (2011), "Novel techniques for human-induced loading experiment and data processing", *Proceeding of the International Symposium on Innovation & Sustainability of Structures in Civil Engineering*, Xiamen, China, October.
Wu, W., Dasgupta, S., Ramirez, E.E. *et al*. (2012), "Classification accuracies of physical activities using smartphone motion sensors", *J. Med. Internet. Res.*, **14**(5), e130.
Yoshida, J., Fujino, Y. and Sugiyama, T. (2007), "Image processing for capturing motions of crowd and its application to pedestrian-induced lateral vibration of a footbridge", *Shock. Vib.*, **14**(4), 251-260.
Yu, Y., Han, R., Zhao, X. *et al.* (2015), "Initial validation of mobile-structural health monitoring method using smartphones", *Int. J. Distrib.Sens. N.*.
Zhang M.S., Chen, J., Peng, Y.X. and Wang, L. (2013), "Reproduction and simulation of walking induced load via motion capture technique and inverse dynamics of rigid body models", *J. Basic Sci. Eng*., **21**(5), 961-972 (in Chinese).
Zhang, M., Gong, W., Li, Z. *et al*. (2007), "Design of remote monitoring system for household appliances and home security based on smart phone", *Meas. Control. Tech.*, **8**, 024.